

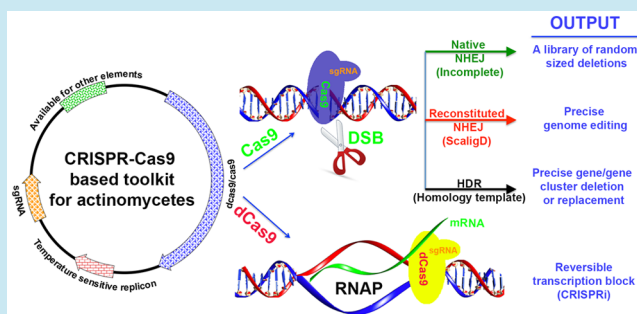
CRISPR-Cas9 Based Engineering of Actinomycetal Genomes

Yaojun Tong,[†] Pep Charusanti,^{†,‡} Lixin Zhang,^{||} Tilmann Weber,^{*,†} and Sang Yup Lee^{*,†,§}[†]The Novo Nordisk Foundation Center for Biosustainability, Technical University of Denmark, Kogle Alle 6, Hørsholm 2970, Denmark[‡]Department of Bioengineering, University of California, San Diego, La Jolla, California 92093, United States[§]Metabolic and Biomolecular Engineering National Research Laboratory, Department of Chemical and Biomolecular Engineering (BK21 Plus Program), Center for Systems and Synthetic Biotechnology, Institute for the BioCentury, Korea Advanced Institute of Science and Technology (KAIST), Daejeon 305-701, Republic of Korea^{||}Chinese Academy of Sciences, Key Laboratory of Pathogenic Microbiology and Immunology, Institute of Microbiology, Beijing 100190, China

S Supporting Information

ABSTRACT: Bacteria of the order *Actinomycetales* are one of the most important sources of pharmacologically active and industrially relevant secondary metabolites. Unfortunately, many of them are still recalcitrant to genetic manipulation, which is a bottleneck for systematic metabolic engineering. To facilitate the genetic manipulation of actinomycetes, we developed a highly efficient CRISPR-Cas9 system to delete gene(s) or gene cluster(s), implement precise gene replacements, and reversibly control gene expression in actinomycetes. We demonstrate our system by targeting two genes, *actIORF1* (SCO5087) and *actVB* (SCO5092), from the actinorhodin biosynthetic gene cluster in *Streptomyces coelicolor* A3(2). Our CRISPR-Cas9 system successfully inactivated the targeted genes. When no templates for homology-directed repair (HDR) were present, the site-specific DNA double-strand breaks (DSBs) introduced by Cas9 were repaired through the error-prone nonhomologous end joining (NHEJ) pathway, resulting in a library of deletions with variable sizes around the targeted sequence. If templates for HDR were provided at the same time, precise deletions of the targeted gene were observed with near 100% frequency. Moreover, we developed a system to efficiently and reversibly control expression of target genes, deemed CRISPRi, based on a catalytically dead variant of Cas9 (dCas9). The CRISPR-Cas9 based system described here comprises a powerful and broadly applicable set of tools to manipulate actinomycetal genomes.

KEYWORDS: CRISPR-Cas9, CRISPRi, DNA repair, actinomycetes, genome engineering



Actinomycetes are Gram-positive bacteria with the capacity to produce a wide variety of medically and industrially relevant secondary metabolites,^{1–3} including many well-known antibiotics, herbicides, chemotherapeutics, and immunosuppressants, such as vancomycin, bialaphos, doxorubicin, and rapamycin, respectively. It is very challenging to find novel secondary metabolites with properties suitable as drug leads as the same known molecules are often rediscovered repeatedly when using traditional approaches. However, there currently is a renaissance in investigating this group of bacteria as studies employing modern genome mining techniques⁴ indicate that they still harbor a huge unexploited potential to produce secondary metabolites with novel structures.⁵ One of the main challenges of this genome-driven approach is to metabolically engineer the strains to express the biosynthetic pathways and to produce the compounds in high titers.⁶ Unfortunately, genetic manipulation of actinomycetes is much more difficult compared to model organisms, such as *Escherichia coli* and *Saccharomyces cerevisiae*, due in part to their more diverse genomic contents

and the extremely high GC content of their genomes. The common gene replacement technique for actinomycetes uses RecA mediated double-crossover events with nonreplicative or temperature sensitive plasmids.⁷ While the efficacy of this approach has been drastically increased by using templates with very long homology regions, such as in the “ReDirect method”,⁸ or using meganuclease I-SceI to introduce DNA DSBs as an additional positive selection marker,⁹ the protocols still are labor-intensive and relatively slow.

In other organisms, several alternative methods that allow precise genome editing have been developed. For example, zinc finger nucleases can be engineered to target custom sequences in human cell lines.¹⁰ Transcription activator-like effectors (TALEs) are another example; they possess a highly modular DNA binding motif that can be engineered to bind to specific sequences in the target genomes.¹¹ More recently, genetic

Received: February 22, 2015

Published: March 25, 2015

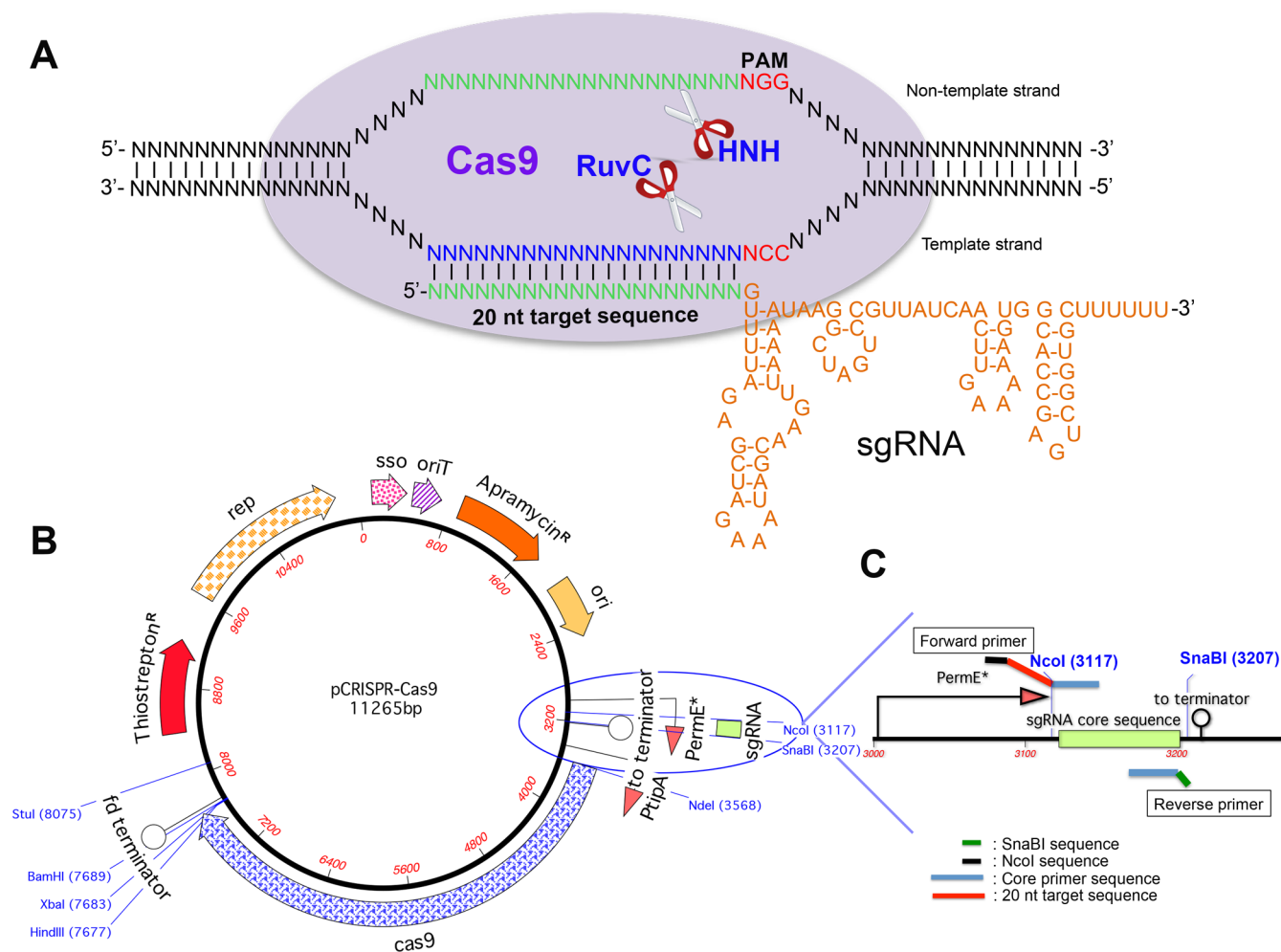


Figure 1. Schematic illustration of the CRISPR-Cas9 system. (A) Diagram of the Cas9 and sgRNA complex. The Cas9 HNH and RuvC-like domains each cleave one strand of the sequence targeted by the sgRNA; the PAM is shown in red; the 20 nt target sequence is shown in green; the sgRNA core structure is shown in orange. (B) Map of pCRISPR-Cas9, the backbone is a temperature sensitive pSG5 replicon, *cas9* is controlled by the thiostrepton inducible *tipA* promoter, the sgRNA cassette is under control of the *ermE** promoter, apramycin serves as the selection marker. This plasmid can shuttle between *E. coli* and actinomycetes. (C) Magnification of the design of sgRNA scaffold in pCRISPR-Cas9.

manipulation systems based on the clustered regularly interspaced short palindromic repeats (CRISPR)/CRISPR-associated (Cas) proteins belonging to the bacterial adaptive immune system have garnered widespread attention. There are three different types of CRISPR systems.¹² Type I and type III CRISPR systems require multiple Cas proteins to induce the cleavage of their target DNA. Type II CRISPR systems, such as those found in *Streptococcus pyogenes*, in contrast only require a single Cas protein, Cas9 (an endonuclease), for activity. The target sequences are defined in the CRISPR loci containing short repeats separated by “spacer” sequences that exactly match the genomes of bacteriophages and other mobile genetic elements offering adaptive immunity to the previously exposed bacteriophages or other mobile genetic elements, and thus are regarded as bacterial adaptive immune systems.^{13–17} In the native type II CRISPR system, the spacer sequence of the CRISPR array transcribes to CRISPR RNA (crRNA). Subsequently, an associated *trans*-activating CRISPR RNA (tracrRNA) hybridizes with the crRNA, forming an RNA duplex, which is cleaved and further processed by endogenous RNase III and possibly other, yet unknown nucleases.¹⁸ The crRNA-tracrRNA duplex interacts with Cas9 to form a complex, and scans the target genome for the presence of

trinucleotide protospacer adjacent motifs (PAMs) (Figure 1A). When this complex finds a PAM that has a 5' sequence complementary to the spacer sequence in the crRNA-tracrRNA duplex, it binds to this position and then triggers the nuclease activity by activating the HNH and RuvC domains of Cas9.^{19,20}

In further studies, Cas9 has shown to be a highly versatile tool to also introduce DNA DSBs into other genomic DNA by coexpression with customized single guide RNAs (sgRNAs), which are artificially generated chimeras of the crRNA and the tracrRNA found in the native CRISPR systems¹⁷ (Figure 1A). This engineered type II CRISPR is referred to as CRISPR-Cas9 system.²¹ Because of its modularization and easy handling, the CRISPR-Cas9 system has been successfully applied as a genome editing tool in a wide range of organisms such as *S. cerevisiae*,²² some plants,²³ *Caenorhabditis elegans*,²⁴ *Drosophila*,²⁵ Chinese hamster ovary (CHO) cells,²⁶ mice,²⁷ rats,²⁸ rabbits,²⁹ and human cells.³⁰ Studies also demonstrated that the CRISPR-Cas9 system can be multiplexed by introducing a battery of sgRNAs that simultaneously target multiple different regions in the genome.³¹ Recently, a CRISPR based system, pCRISPMycetes was developed for streptomycetes genetic manipulation.³² However, this method only harnesses the DSBs introduced by Cas9 nuclease to mediate the homologous

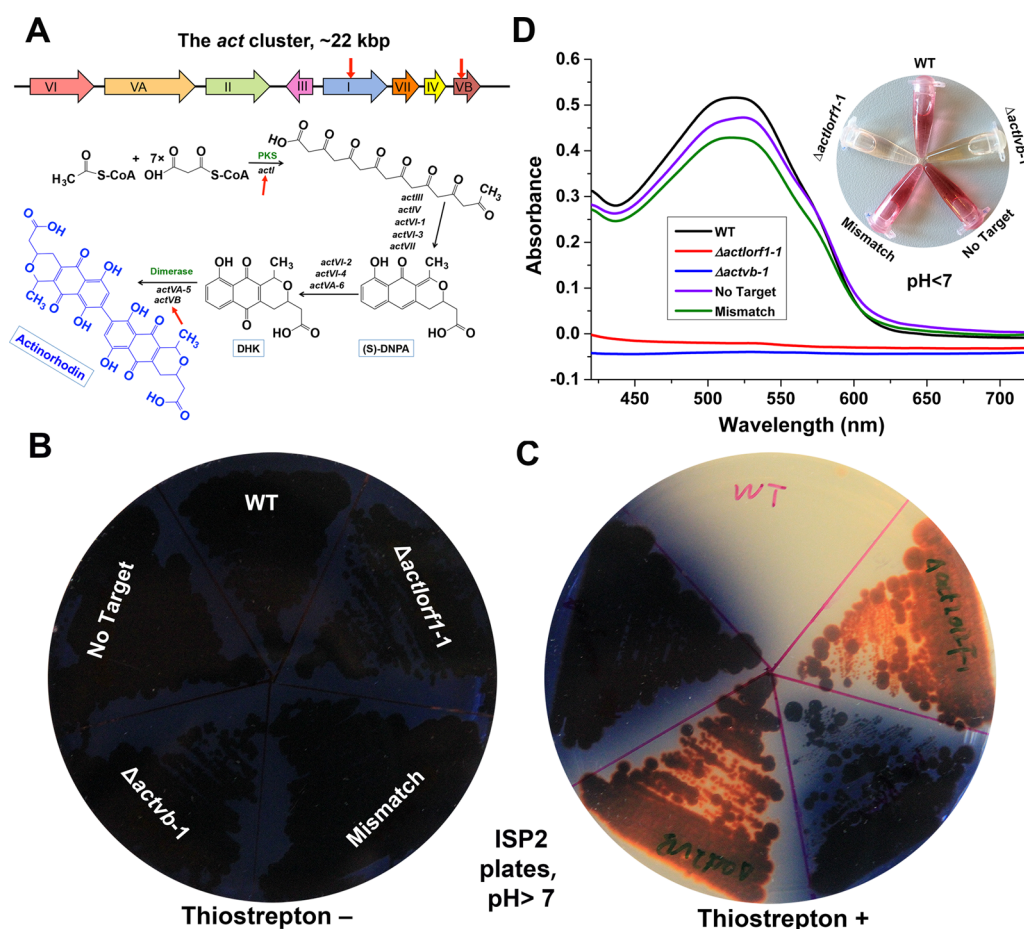


Figure 2. Actinorhodin biosynthetic pathway was inactivated by CRISPR-Cas9. (A) Organization of the actinorhodin biosynthetic gene cluster. For clarity, genes of the same functional group are summarized as one arrow. For the detailed actinorhodin biosynthesis, please see review.⁵⁸ (B) ISP2 plate without antibiotics. All five strains are blue. (C) ISP2 plate with 1 $\mu\text{g/mL}$ thiostrepton. Labels correspond to those in B. The blue from strains $\Delta\text{actIorf1-1}$ and $\Delta\text{actvb-1}$ disappeared. The photos were taken after 7 days incubation at 30 $^{\circ}\text{C}$. (D) Actinorhodin detection by UV-visible spectrometry. When the pH is lowered to 2, actinorhodin turns from blue to red, and has a maximum absorption at about 530 nm. See Methods for further details.

recombination events, but does not fully implement the features of CRISPR-Cas9 system.

Besides introduction of DSBs, it was shown that mutating the HNH and RuvC domains of Cas9 (D10A and H840A) resulted in a catalytically dead Cas9 (dCas9) that did not have endonuclease activity, but could still form a complex with sgRNA and efficiently bind to the target DNA.¹⁷ This effect can be used to sequence-specifically interfere with transcription and thus control gene expression. In analogy to eukaryotic RNA interference RNAi, this system was named as CRISPRi.³³

Here we report a CRISPR-Cas9 system for manipulation of actinomycetal genomes. As in the previous report,³² our system can be used to create precise deletions in the genomes of streptomycetes *via* double-crossover with homologous recombination templates. Moreover, we report additional capabilities of our system, specifically that it functions even in the absence of homology templates, which results in a distribution of fragment deletion sizes, and that it can be redesigned to reversibly control gene expression.

RESULTS AND DISCUSSION

Design of a One Plasmid-Based CRISPR-Cas9 System.

The temperature sensitive vector pGM1190, a derivative of pGM190,³⁴ whose selection marker is apramycin instead of

kanamycin, was used as a backbone to harbor both components of our CRISPR-Cas9 system, the nuclease Cas9/dCas9 and the “homing device” sgRNA, which was constructed by fusing a crRNA and an associated tracrRNA¹⁷ (Figure 1A). The replication systems of this *E. coli*-actinomycetes shuttle vector are based on pMB1 and pSG5.³⁵ The nuclease Cas9/dCas9 is under control of the thiostrepton inducible *tipA* promoter, which requires the presence of the thiostrepton responsive activator TipA.³⁶ The gene encoding this protein, *tipA*, is not present in pGM1190, but is present in the genomes of most *Streptomyces*, including *Streptomyces coelicolor*.³⁷ Therefore, it would be necessary to clone *tipA* into pGM1190 or change the promoter system prior to the use of our system in actinomycetes lacking a native *tipA* gene. For easy handling, the 20 nt target sequence within the sgRNA scaffold was designed to be inserted into the *NcoI* and *SnaBI* restriction sites (Figure 1C). The *StuI* restriction site within the pCRISPR-Cas9 vector is available for inserting other elements (Figure 1B), for instance to subclone a homologous recombination template for precise gene deletion, or the ScaligD expression cassette to reconstitute the incomplete NHEJ pathway. Because of its temperature sensitivity, the plasmids can be eliminated from actinomycete cells by incubating cells above 34 $^{\circ}\text{C}$.

Actinorhodin Biosynthesis Was Successfully Interrupted by Targeting Genes within the Pathway with the CRISPR-Cas9 System. To validate the CRISPR-Cas9 system, we chose to inactivate two genes, *actIORF1* and *actVB*, from the biosynthetic pathway of the blue-pigmented polyketide antibiotic actinorhodin in *S. coelicolor* (Figure 2A). sgRNAs were identified with a modified version of the software CRISPRy²⁶ (http://staff.biosustain.dtu.dk/laeb/crispy_scoeli/). On the basis of the predictions, 6 sgRNAs with no predicted off-target effects were selected for each of the two genes (Table S3, Supporting Information). The sgRNAs were subcloned into pCRISPR-Cas9, and after sequence validation, one correct plasmid for each sgRNA was randomly selected to be transferred into the ET12567/pUZ8002 *E. coli* strain for conjugation. No template for HDR was used at this stage. In addition, three negative controls were used. The first one was an “empty vector” in which the 20 nt target sequence of sgRNA is missing, resulting in no expected target match in the genome. This control was named “No Target”. The second one contained a 23 nt sgRNA composed of the 20 nt target sequence of *actIORF1* extended by the 3 nt PAM motif “NGG”. The inclusion of the PAM as part of the sgRNA abolishes correct recognition of the genomic target and therefore was called “Mismatch”. The last one is the wild-type (WT).

After conjugation, 30–80 colonies transformed with each sgRNA were randomly picked onto two different sets of ISP2 plates. Only one set was supplemented with 1 μ g/mL thioestrepton that induces Cas9 expression. The ratio of clones that lost actinorhodin production over the total number of clones on the induction plates was used to calculate the efficiency for each sgRNA. The inactivation efficiency varied from 3 to 54%, depending on the different sgRNAs (Table 1).

Table 1. Inactivation Efficiency of Different sgRNAs with Different DSB Repair Pathways

ways of DSB repair	sgRNAs	colony count ^a				efficiency (%)
		no growth	red ^b	blue	total	
incomplete NHEJ	ActIorf1-1 NT	20	31	30	81	38
	ActIorf1-2 T	3	1	7	11	9
	ActIorf1-3 T	7	18	49	74	24
	ActIorf1-4 T	43	10	1	54	19
	ActIorf1-5 T	8	18	8	34	53
	Actvb-1 NT	10	20	22	52	38
	Actvb-3 T	17	6	40	63	10
	Actvb-4 T	30	6	5	41	15
	Actvb-5 NT	7	20	10	37	54
	Actvb-6 NT	1	1	30	32	3
	ActIorf1-6 T	10	18	12	40	45
	Actvb-2 NT	20	13	2	35	37
	reconstituted NHEJ	ActIorf1-6 T	0	24	7	31
Actvb-2 NT		0	18	8	26	69
HDR (with homology templates)	ActIorf1-6 T	0	52	0	52	100
	Actvb-2 NT	0	35	1	36	97

^aDenotes the number of colonies with the indicated phenotype after induction with thioestrepton. ^bActinorhodin is blue. Upon loss of actinorhodin production, the red color of the 2nd pigmented antibiotic, undecylprodigiosin, becomes visible.

Two clones for each target gene that lost blue pigment formation after induction were randomly selected, named $\Delta actIorf1-1$, $\Delta actIorf1-2$ and $\Delta actvb-1$, $\Delta actvb-2$, respectively, and were further investigated together with the three negative controls, “No Target”, “Mismatch”, and the WT (Table S1). When they were transferred to new agar plates without the inducer thioestrepton, still no blue pigment was observed for the strains carrying sgRNAs targeting *actIORF1* and *actVB*, while the control strains were dark blue (only $\Delta actIorf1-1$, $\Delta actvb-1$ and 3 controls are shown in Figure 2, and Figure S1). The visual analysis on the agar plates was also confirmed by cultivating the clones in liquid ISP2 medium and detecting actinorhodin production with UV–visible spectroscopy (Figure 2D). These observations indicated that the CRISPR-Cas9 system indeed inactivated the *actIORF1* and *actVB* genes, so that the actinorhodin biosynthesis was interrupted.

As mentioned above, the efficiency with which the different sgRNAs yielded clones with abolished actinorhodin production varied from 3 to 54% (Table 1). This low efficiency was due to the absence of a homology-directed repair template. Survival was most likely due to repair of the DNA DSBs with the imperfect NHEJ pathway.

Random Sized Deletions Caused by Imperfect NHEJ in Actinomycetes. To unambiguously confirm that the observed phenotype is due to the targeted inactivation of the two actinorhodin biosynthetic genes, but not due to unwanted side- or off-target effects, we sequenced the whole genomes of the above selected 7 strains using Illumina technology in order to map the sites of mutation. Comparison of the *S. coelicolor* A3(2) strain used in this study (WT) with the *S. coelicolor* A3(2) reference sequence (Genbank: AL645882), resulted in 95 SNPs (Table S4) and 1 fragment (5797650–5818686) deletion, which corresponds to the loss of an integrated plasmid in our WT strain. Subsequently, the sequence of our WT strain was used as the mapping reference for the other strains. The detailed mapping results of the analysis are shown in Table S5 and Figure 3A.

Interestingly, the whole genome sequencing analysis indicated the inactivation of *actIORF1* and *actVB* was not uniform. In one of the investigated clones where *actIORF1* was targeted, the inactivation was caused by a 1 bp insertion (Figure 3B). In another case (*actVB* was targeted), a deletion of more than 30 000 bp around the DSB position was obtained (Figure 3A). In other words, the deletions were precisely placed at the targeted sites, but varied in size. Importantly, this observation confirmed that a NHEJ pathway indeed exists in actinomycetes, but its efficiency is much lower than in eukaryotic organisms.^{38,39} Thus, this feature can be exploited to easily generate a set of random-sized deletions around a precisely defined target position through a single experiment using the CRISPR-Cas9 system.

Optimizing the Intrinsic NHEJ Pathway by Coexpression of a LigD Ligase. It was hypothesized that the efficiency of the CRISPR-Cas9 system could be improved in *S. coelicolor* by coexpressing a DNA ligase D (LigD). Analysis of actinomycetal genome sequences showed that most actinomycetes lack LigD, a core component of the NHEJ pathway, which is present, for example, in *Mycobacterium tuberculosis*.

A BLAST search using the *M. tuberculosis* LigD (MtbligD) as a query against the NCBI nonredundant database revealed that there currently is only one known LigD homologue of streptomycete origin, which is found in *Streptomyces carnes* (NCBI GenPept ID WP_033244577.1). The amino acid

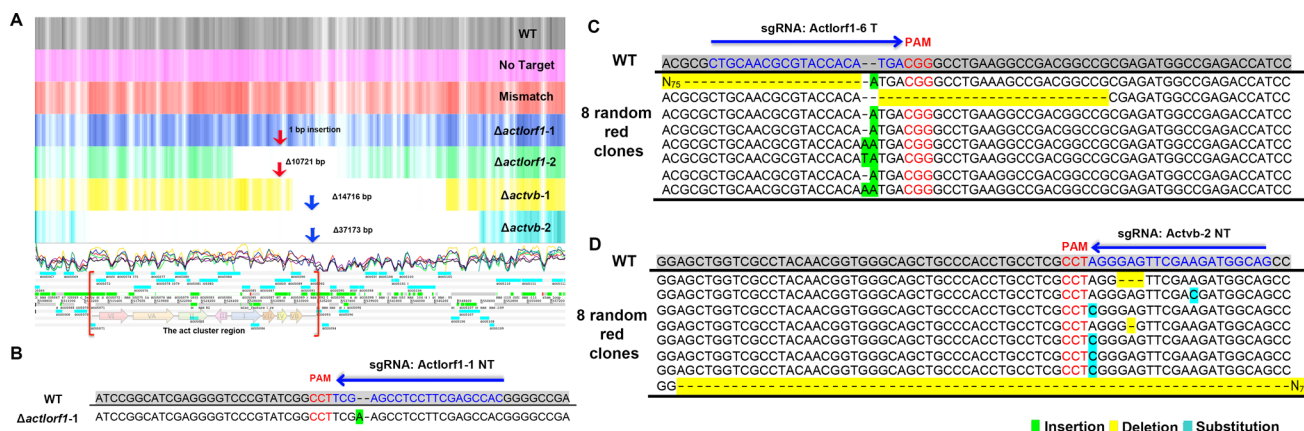


Figure 3. Analysis of the sequencing data. (A) Heatmap of the 7 mapped sequencing samples to the *S. coelicolor* A3(2) reference genome in a native NHEJ system. Dark colors represent a high read coverage, white represents low/no coverage. Displayed is the region spanning 5508800 to 5557230 of the *S. coelicolor* genome. The actinorhodin gene cluster is denoted by red brackets; the target sites of the *actIORF1* and *actVB* sgRNAs are displayed as red and blue arrows. The deletion sizes are shown on the map. (B) Alignment of the sequence traces of $\Delta actIorf1-1$ with the WT. The blue arrow indicates the genomic target site of the sgRNA: ActIorf1-6 T. The PAM sequence is shown in red. (C, D) DNA sequences of 8 randomly selected red clones aligned to the WT genomic sequence of *actIORF1* and *actVB*, respectively, in a reconstituted NHEJ system. The blue arrow indicates the genomic target sites of the related sgRNAs. The PAM sequences are shown in red. Green, yellow and light blue colors indicate insertions, deletions and substitutions, respectively.

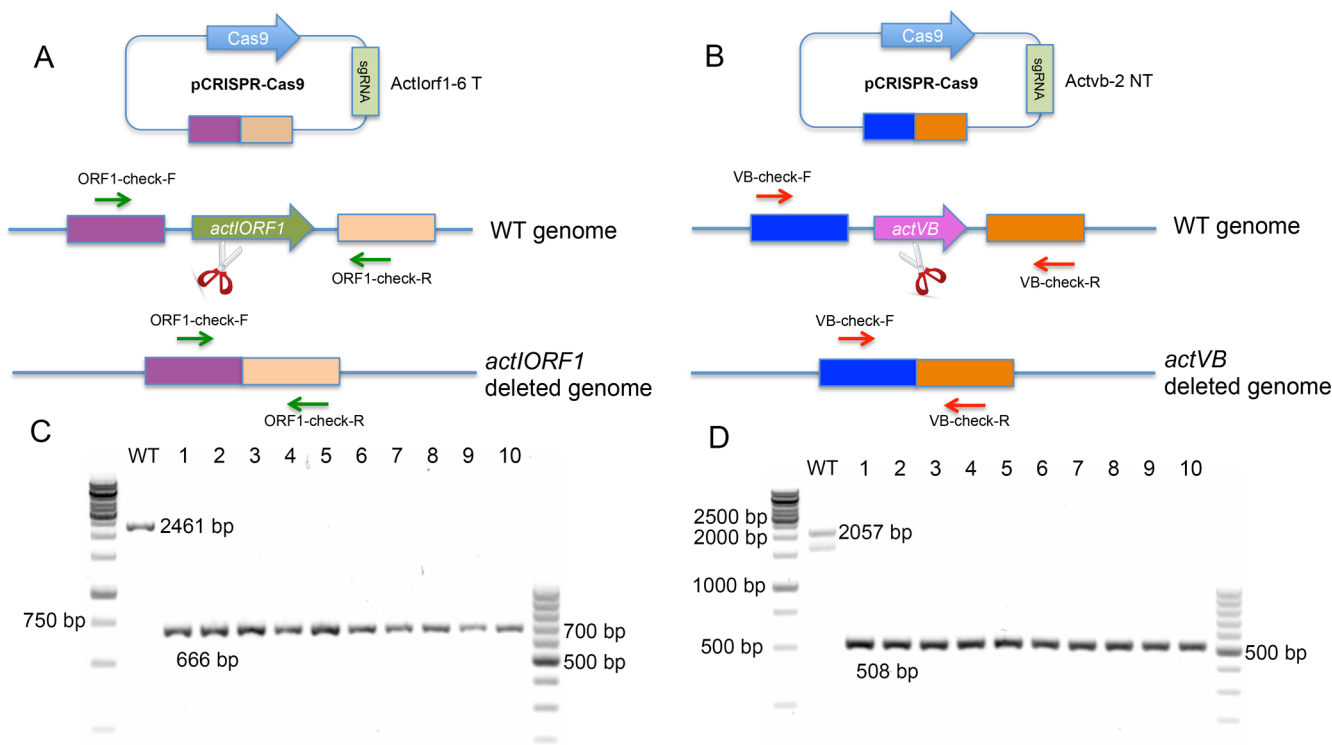


Figure 4. HDR pathway to repair the DNA DSBs caused by CRISPR-Cas9 system. (A, B) Diagrams of the CRISPR-Cas9 vectors with homologous recombination templates for *actIORF1* and *actVB*. (C, D) Colony PCR of 10 randomly selected clones that lost actinorhodin production to confirm deletion of *actIORF1* (C) and *actVB* (D) after use of the two vectors in A and B.

identity and similarity to MtblgD is 56 and 67%, respectively. To coexpress it in our CRISPR-Cas9 system, the expression cassette ScaligD was designed. An internal *NcoI* site was removed from the *S. carneus ligD* gene by introducing the synonymous substitution C606G. The construct was synthesized by Genscript and subcloned into the *StuI* site of pCRISPR-Cas9 by Gibson assembly. This modified system together with one sgRNA for each of the two target genes (sgRNA: ActIorf1-6 T for *actIORF1*, and sgRNA: Actvb-2 NT

for *actVB*) were used to investigate how the inclusion of ScaligD affected the inactivation efficiency; the efficiency increased from 45 to 77% for the sgRNA ActIorf1-6 T and from 37 to 69% for Actvb-2 NT (Table 1). To further validate the observation, primers were designed to amplify the ~600 bp fragment containing the theoretical cleavage sites of the used sgRNAs. Eight red clones for each gene were randomly selected for colony PCR and subsequent Sanger sequencing. No large deletions were found in any the 16 sequenced clones; most had

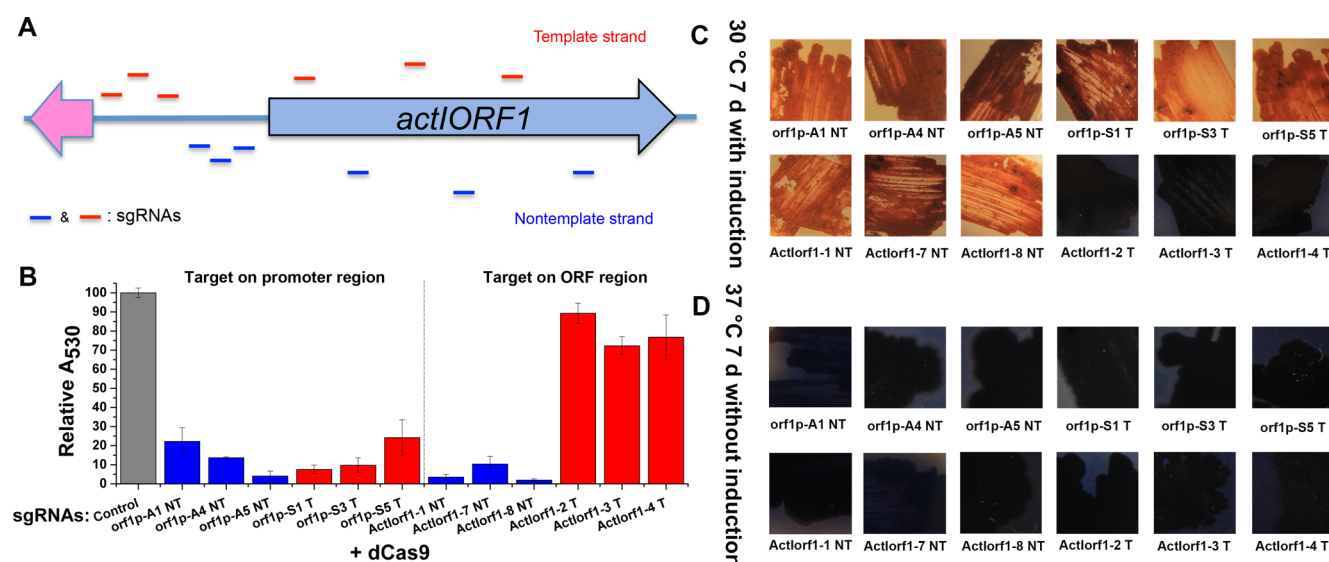


Figure 5. CRISPRi effectively silences *actIORF1* expression in a reversible manner. (A) Location of the 12 sgRNAs for CRISPRi. Half were designed to target the promoter region, while the other half were designed to target the ORF. In addition, half target the template strand and half target the nontemplate strand. (B) The 530 nm absorbance of extracts from cultures tested with the 12 sgRNAs shown in A relative to the wild-type control. Mean values from three independent extractions are shown. Error bars represent the standard deviation from three independent extractions. (C, D) Reversibility of the CRISPRi system. Red clones become blue when the incubation temperature is increased to 37 °C, indicating that the CRISPRi effect has gone away.

1 to 3 bp deletions, substitutions, or insertions (Figure 3C, and Figure 3D). For comparison, three out of four clones that lost actinorhodin production were found to have large deletions when ScaligD was not included (Figure 3A). These results indicated that the incomplete NHEJ pathway was successfully reconstituted by complementing the missing DNA ligase D.

Precise Gene Deletion in Actinomycetes Using HDR.

We next investigated whether the presence of a homologous recombination template could improve the efficiency and fidelity of the CRISPR-Cas9 system even further, as homologous recombination is used regularly to target gene replacement and deletion in a wide range of organisms including actinomycetes.⁴⁰ A ~2.2 kbp homologous recombination template for each of the two target genes (*actIORF1* and *actVB*) was amplified by PCR, assembled and subcloned into the *StuI* site of pCRISPR-Cas9. The same sgRNAs (sgRNA: Actlorf1-6 T for *actIORF1*, and sgRNA: Actvb-2 NT for *actVB*) were selected for testing. All 52 clones randomly picked for *actIORF1*, and 35 out of 36 clones randomly picked for *actVB* lost actinorhodin production after induction (Table 1). Ten red clones were randomly selected for colony PCR validation for both genes. The sizes of all 20 PCR products obtained in the reactions corresponded to the predicted sizes of the gene deletion (Figure 4), which were confirmed by Sanger sequencing. Importantly, the CRISPR-Cas9 system using the homologous recombination templates showed even higher efficiency and precision when compared to the gene deletion system involving ScaligD (Table 1).

An Effective and Reversible CRISPRi System for Gene Expression Controls in *S. coelicolor*. In some instances, the reversible repression of gene expression is preferred over gene deletion. As such, we tested whether a modified system, referred to as CRISPRi, could be adapted for use to control gene expression in actinomycetes. Again, the *actIORF1* gene was selected as the test case. Since the CRISPRy software used to identify sgRNAs for gene deletion can only identify target sequences within the coding regions, a different sgRNA finder

software, sgRNACas9,⁴¹ was used to identify the sgRNAs from noncoding regions for the CRISPRi system. Six sgRNAs that targeted the promoter region and another six targeting the ORF of *actIORF1* were selected. In both cases, three of six targeted the template strand DNA and the other three targeted the nontemplate strand (Table S3 and Figure 5A). In clones carrying sgRNAs targeting the promoter region, actinorhodin production was abolished or dramatically reduced regardless of whether they targeted the template or nontemplate strand. In clones carrying sgRNAs that targeted the ORF region, loss of or reduced actinorhodin production was only observed when the sgRNAs targeted the nontemplate strand (Figure 5B, C). To test whether the effect was reversible, the loss of the pCRISPR-dCas9 plasmid was induced by increasing the incubation temperature to 37 °C for 24 h and then transferring the cultures to fresh ISP2 plates without antibiotic selection. After incubation for 5 days at 37 °C, the colonies had regained their dark blue color (Figure 5C, D), indicating that the repression of actinorhodin biosynthesis by the CRISPR-dCas9 (CRISPRi) system was abrogated and all genes of the actinorhodin biosynthetic pathway were expressed again.

Discussion. The classical method for actinomycete gene manipulation is double-crossover based gene replacements with nonreplicative or temperature sensitive plasmids.⁷ The efficiency of the mutagenesis can be highly improved by using long homology regions in the gene inactivation plasmids.⁸ In this protocol, cosmids/fosmids with inserts covering the target region are engineered in *E. coli* using Rec/ET recombineering and then used as very long templates (up to 20 kbp homology arms) for homologous recombination mediated gene replacement. Although this method increases the frequency of obtaining double-crossovers significantly, the generation of such constructs is very laborious and the overall efficiency is still relatively low. Thus, alternative systems are of great interest for the actinomycetes research community.

One system that has gained recent attention is based on CRISPR-Cas9, which is an antiphage defense mechanism in

bacteria and archaea. Two core components of this system are the nuclease Cas9 and its “homing device” sgRNA. The sgRNA sequence originally corresponded to phage sequences, but it has been shown that it can be replaced by a sequence of interest to reguide the Cas9 nuclease for genome editing.²¹ Because of its modularity and simplicity, CRISPR-Cas9 system has been successfully adapted for genome editing in an increasing number of organisms, mainly eukaryotic hosts and some bacteria.³²

We observed nearly 100% efficiency in precise gene deletion in *S. coelicolor* when CRISPR-Cas9 was used in tandem with a homology-based repair template (Figure 4). The observed efficiency is in very good agreement with data reported from the recently developed pCRISPRomyces-system,³² another CRISPR-based system for actinomycetes that uses a similar strategy.

DNA DSBs of the chromosome are lethal events in both prokaryotic and eukaryotic organisms unless the lesion is repaired by HDR or NHEJ.^{42,43} Therefore, the use of CRISPR-Cas9 to cleave the host's chromosome was recently proposed as an antimicrobial application^{44–47} as many pathogenic bacteria cannot repair chromosomal DSBs by NHEJ. However, in this study, we observed that *S. coelicolor* can survive after the DNA DSBs introduced by Cas9 even in the absence of a homologous recombination template. Resulting colonies, however, contained deletions of variable sizes around the target site. In our study for instance, one single sgRNA generated deletions ranging from 1 bp to more than 10 000 bp. This property can be exploited and used to generate a set of random sized deletions originating from a single sgRNA-directed target on the genome, which would be valuable to generate genome minimized hosts or to identify essential genes in actinomycetes. When a DNA ligase D homologue from *S. carneus* was coexpressed, the efficiency of the NHEJ pathway was significantly improved. This enables the use of the CRISPR-Cas9 system in an analogous way as in eukaryotes, where no homologous template has to be provided to generate targeted mutations.

In addition to using CRISPR-Cas9 system as a genome editing tool, it has recently been engineered to transiently control gene expression, a system referred to as CRISPRi in analogy to the eukaryotic RNAi technology. It was shown that two single amino acid substitutions in Cas9 (D10A and H840A) result in Cas9 variants that lack the endonuclease activity but retain the ability to target DNA depending on the coexpressed sgRNA. This targeted binding, which no longer results in DSBs, can now be used to sterically block transcription.³³ By introducing the modifications (D10A and H840A) into our CRISPR-Cas9 system, it was possible to efficiently knock down gene expression in *S. coelicolor*. The CRISPRi we describe here does not rely on complex regulation factors but only requires the dCas9 protein and an sgRNA to control the expression of the target gene(s) of actinomycetes. Because of the easy cloning procedures required to generate the CRISPRi plasmids, this system is well suited as an alternative to the other tools available to control gene expression in actinomycetes, for example the integration of heterologous promoters, riboswitches,⁴⁸ or using antisense RNA.⁴⁹ As our system is encoded on a temperature sensitive plasmid under the control of an inducible promoter, the repression can be easily induced and removed by eliminating the plasmid. Besides the gene silencing effects of CRISPRi, it can also be extended to other applications. For instance, combining it with a blue light

sensor allows for quantitative interrogation of cellular activities,⁵⁰ and together with the CRISPR activators (CRISPRa) system it can enable systematic investigation of the cellular consequences of repressing or inducing individual transcripts, which can provide rich and complementary information for mapping complex pathways.⁵¹

It is expected that the CRISPR-Cas9 gene deletion system and the CRISPRi based gene expression control system developed in this study will accelerate the metabolic engineering of actinomycetes, mutational/expression analyses of specific biosynthetic pathways, the *in vivo* generation of secondary metabolite derivatives, and the creation of genome minimized platform strains for heterologous expression of biosynthetic gene clusters (Figure S2). The system will be readily applicable also to other streptomycetes and related actinomycetes.

METHODS

Strains, Plasmids, Media and Growth Condition. The strains and plasmids used in this study are listed in Table S1. *S. coelicolor* strains were grown in ISP2 medium (agar and liquid), and conjugation was carried out on mannitol soya flour (MS) agar supplemented with 10 mM MgCl₂. *E. coli* strains were grown in LB medium (agar and liquid). Appropriate antibiotics were added to the media when needed at the following concentrations: apramycin, 50 μg/mL; nalidixic acid, 50 μg/mL; thiostrepton, 1 μg/mL; kanamycin, 25 μg/mL and chloramphenicol, 25 μg/mL.

Construction of the CRISPR-Cas9 Vectors. The CRISPR-Cas9 system includes 2 different vectors: pCRISPR-Cas9 for gene deletion or replacement, and pCRISPR-dCas9 for gene expression control. The temperature sensitive plasmid pGM1190³⁵ was selected as the backbone. The sgRNA scaffold was designed by fusing tracrRNA and crRNA into a chimeric sgRNA.¹⁷ The 20 nt target sequence within the sgRNA scaffold is flanked by two unique restriction sites, *NcoI* and *SnaBI*, to allow facile insertion. Expression of the sgRNA is under control of the constitutive *ermE** promoter. The sgRNA scaffold was subcloned into the *SnaBI* site of pGM1190 using Gibson assembly in front of the *to* terminator, named pCRISPR-sgRNA. The *to* terminator served as a secondary terminator for the sgRNA scaffold. The *cas9* used in our system has been codon optimized using Genscript's OptimumGene algorithm to account for the large difference in the GC content (35 vs 72%) and codon bias between *S. pyogenes* and *S. coelicolor*. The optimized *cas9* was subcloned into pGM1190-sgRNA with *NdeI* and *XbaI* sites, under control of the thiostrepton inducible *tipA* promoter,⁵² resulting in the final construct: pCRISPR-Cas9. To utilize the CRISPRi effects for gene expression control, both nuclease domains (the RuvC1 and the HNH) in the codon optimized *cas9* gene were mutated (D10A and H840A),¹⁷ resulting in a catalytically dead variant (dCas9) without endonuclease activity. The Cas9 of the pCRISPR-Cas9 was replaced by dCas9, resulting in pCRISPR-dCas9, which used for CRISPRi system. In order to reconstitute the incomplete NHEJ pathway, a ScaligD expression cassette was designed and synthesized by Genscript, which is under control of an *ermE** promoter, and with a *to* terminator. This expression cassette was amplified by the primers ScaligD-F and ScaligD-R (Table S2), then subcloned into the *StuI* site of pCRISPR-Cas9 by Gibson assembly to make pCRISPR-Cas9-ScaligD.

The only requirement to use our CRISPR-Cas9 related plasmids is insertion of the 20 nt target sequence into the

sgRNA scaffold, which can be achieved by changing the N20 region of the forward primer (sgRNA-F) CATGCCATGG-N₂₀GTTTTAGAGCTAGAAATAGC (N₂₀ represents the 20 nt target sequence). The reverse primer (sgRNA-R) always remains the same (Table S2). PCR was used to generate the sgRNA with target sequence using pCRISPR-Cas9 as the template. Then, the PCR product was digested with *Nco*I and *Sna*BI, and ligated to *Nco*I and *Sna*BI predigested pCRISPR-Cas9, pCRISPR-Cas9-ScaligD, or pCRISPR-dCas9. All the plasmids were maintained in Mach1-T1 *E. coli* (Life Technologies, U.K.). The N₂₀ target sequences were identified by *S. coelicolor* modified version of CRISPy;²⁶ http://staff.biosustain.dtu.dk/laeb/crispy_scoeli/, and sgRNAs9.⁴¹ The list of the sgRNAs used in this study is shown in Table S3. The relevant primers used to construct the functional sgRNA are shown in Table S2. The plasmids were transferred into *S. coelicolor* A3(2) by conjugation. Colony PCR and Sanger sequencing were performed to screen for the correct constructs.

Construction of Homologous Recombination Templates. PCR was used to amplify the ~1 kbp fragments of the 5' and the 3' regions out of the targeted genes with the primers (Table S2) orf1-5'F, orf1-5'R, orf1-3'F, orf1-3'R, and VB-5'F, VB-5'R, VB-3'F, VB-3'R, for *actIORF1* and *actVB*, respectively. The orf1-5'F and VB-5'F primers contain a 20 bp overhang region of the 5' end of the *Stu*I site from the pCRISPR-Cas9 plasmid, and the orf1-3'R and VB-3'R primers contain a 20 bp overhang region of the 3' end of the *Stu*I site from the pCRISPR-Cas9 plasmid. The orf1-5'R and VB-5'R primers contain a 20 bp overhang of the orf1-3' fragment and VB-3' fragment, respectively. After gel purification of the fragments, orf1-5', orf1-3', and the *Stu*I digested pCRISPR-Cas9 plasmid, and VB-5', VB-3', and the *Stu*I digested pCRISPR-Cas9 plasmid were assembled with the Gibson Assembly kit (New England Biolabs, US). The transformants were screened by colony PCR using primers orf1-check-F, orf1-check-R and VB-check-F, VB-check-R for the homologous recombination templates for *actIORF1* and *actVB*, respectively, and finally confirmed by sequencing.

DNA Manipulation. Primers used in this study are listed in Table S2. Standard procedures were used for DNA purification, PCR, subcloning, and molecular analysis. PCR was performed using Maxima Hot Start Taq DNA Polymerase (Thermo Scientific, US), and Phusion High-Fidelity PCR Kit (Thermo Scientific, US). Other enzymes used in this study were from Thermo Scientific. All kits and enzymes were used according to the manufacturers' recommendations.

Transfer of the Plasmids from *E. coli* to *S. coelicolor* by Conjugation. The relevant plasmids first were transferred into *E. coli* ET12567/pUZ8002 cells by calcium chloride transformation. Conjugation between *E. coli* ET12567/pUZ8002 and *S. coelicolor* A3(2) was carried out as described previously.⁷ The plates were incubated for 3–7 days at 30 °C, or until conjugates became visible.

Genomic DNA Extraction, MiSeq Library Construction, Sequencing and Sequence Analysis. Genomic DNA was extracted from 10 mL culture (shaking for 7 days at 30 °C) for each strain using Blood & Cell Culture DNA Kit (QIAGEN, Germany). The genomic libraries were generated using the TruSeq Nano DNA LT Sample Preparation Kit (Illumina Inc., US). Briefly, 100 ng of genomic DNA diluted in 52.5 μL of TE buffer was fragmented in Covaris Crimp Cap microtubes on a Covaris E220 ultrasonicator (Covaris, U.K.) with 5% duty factor, 175 W peak incident power, 200 cycles/

burst, and 50 s duration under frequency sweeping mode at 5.5 to 6 °C (Illumina recommendations for a 350 bp average fragment size). The ends of fragmented DNA were repaired by T4 DNA polymerase, Klenow DNA polymerase, and T4 polynucleotide kinase. The Klenow exomix enzyme was then used to add an "A" base to the 3' end of the DNA fragments. After the ligation of the adapters to the ends of the DNA fragments, DNA fragments ranging from 300 to 400 bp were recovered by bead purification. Finally, the adapter-modified DNA fragments were enriched by 3 cycle-PCR. Final concentration of each library was measured by Qubit 2.0 Fluorometer and Qubit DNA Broad range assay (Life Technologies, U.K.). Average dsDNA library sizes were determined using the Agilent DNA 7500 kit on an Agilent 2100 Bioanalyzer. Libraries were normalized and pooled in 10 mM Tris-Cl, pH 8.0, plus 0.05% Tween 20 to the final concentration of 10 nM, and denatured in 0.2 N NaOH. A 10 pM pool of 20 libraries in 600 μL of ice-cold HT1 buffer was loaded onto the flow cell provided in the MiSeq Reagent kit v2 (300 cycles) and sequenced on a MiSeq (Illumina Inc., US) platform with a paired-end protocol. The reads obtained from the sequencing of samples were mapped to the *S. coelicolor* A3(2) reference genome⁵³ using the software BWA⁵⁴ with the BWA-mem algorithm. The data was inspected and visualized using readXplorer⁵⁵ and Artemis.⁵⁶

Colony PCR for Actinomycetes. In order to quickly identify the genetic changes in the actinomycetes, mycelia of the selected colonies were scraped from the plates using a sterile toothpick into 10 μL pure DMSO in PCR tubes. The tubes were shaken vigorously for 10 min at 100 °C in a heating block. After this step, the solution was spun down at top speed for 10 s, 1 μL of the supernatant was used as the PCR template in a 20 μL reaction.

Detection of Actinorhodin. This method was modified from Bystrikh et al. (1996).⁵⁷ The *S. coelicolor* clones (from ISP2 plates with thiostrepton) were inoculated in 100 mL ISP2 liquid medium, and incubated with shaking for 7 days at 30 °C. A 30 mL culture for each strain was used to extract actinorhodin. The cultures were centrifuged at 8000g for 10 min at room temperature, the supernatant was transferred to a 50 mL tube, the pH was adjusted to about 2 with 1 M HCl, and then chloroform was added (1/4 volume). The solution was vortexed vigorously and then centrifuged at 8000g for 5 min at room temperature. The chloroform phase was collected, and the solvent was evaporated. The dried samples were redissolved using 2 mL solvent (methanol:chloroform = 1:1). The solutions were analyzed using the Evolution 220 UV–visible Spectrophotometers (Thermo Scientific, US). Actinorhodin had a peak absorption at ~530 nm.

The Genbank accession numbers for the vector pCRISPR-Cas9 and the codon optimized *dcas9* are KR011749 and KR011748, respectively.

■ ASSOCIATED CONTENT

📄 Supporting Information

Five additional tables and two figures. The Supporting Information is available free of charge on the ACS Publications website at DOI: 10.1021/acssynbio.5b00038.

■ AUTHOR INFORMATION

Corresponding Authors

*E-mail: tiwe@biosustain.dtu.dk.

*E-mail: leesy@kaist.ac.kr.

Author Contributions

Y. Tong, T. Weber and S. Y. Lee designed the experiments; Y. Tong performed the experiments; Y. Tong, P. Charusanti and L. Zhang analyzed the data; Y. Tong, T. Weber and S. Y. Lee wrote the manuscript.

Notes

The authors declare no competing financial interest.

ACKNOWLEDGMENTS

This work was funded by a grant from the Novo Nordisk Foundation. S.Y.L acknowledges support from the Intelligent Synthetic Biology Center through the Global Frontier Project (2011-0031963) of the Ministry of Science, ICT & Future Planning through the National Research Foundation of Korea. We thank Günther Muth at University of Tübingen for providing the pGM1190 vector, and Hyun Uk Kim at KAIST for critical discussion.

REFERENCES

- (1) Berdy, J. (2005) Bioactive microbial metabolites—A personal view. *J. Antibiot.* 58, 1–26.
- (2) Berdy, J. (2012) Thoughts and facts about antibiotics: Where we are now and where we are heading. *J. Antibiot.* 65, 385–395.
- (3) Hwang, K. S., Kim, H. U., Charusanti, P., Palsson, B. O., and Lee, S. Y. (2014) Systems biology and biotechnology of *Streptomyces* species for the production of secondary metabolites. *Biotechnol. Adv.* 32, 255–268.
- (4) Blin, K., Medema, M. H., Kazempour, D., Fischbach, M. A., Breitling, R., Takano, E., and Weber, T. (2013) antiSMASH 2.0—a versatile platform for genome mining of secondary metabolite producers. *Nucleic Acids Res.* 41, W204–212.
- (5) Weber, T., Charusanti, P., Musiol-Kroll, E. M., Jiang, X., Tong, Y., Kim, H. U., and Lee, S. Y. (2015) Metabolic engineering of antibiotic factories: new tools for antibiotic production in actinomycetes. *Trends Biotechnol.* 33, 15–26.
- (6) Lee, S. Y., Kim, H. U., Park, J. H., Park, J. M., and Kim, T. Y. (2009) Metabolic engineering of microorganisms: general strategies and drug production. *Drug Discovery Today* 14, 78–88.
- (7) Kieser, T., Bibb, M., Buttner, M., Chater, K., and Hopwood, D. (2000) *Practical Streptomyces Genetics*, John Innes Foundation, Norwich, U.K.
- (8) Gust, B., Chandra, G., Jakimowicz, D., Yuqing, T., Bruton, C. J., and Chater, K. F. (2004) Lambda red-mediated genetic manipulation of antibiotic-producing *Streptomyces*. *Adv. Appl. Microbiol.* 54, 107–128.
- (9) Fernandez-Martinez, L. T., and Bibb, M. J. (2014) Use of the Meganuclease I-SceI of *Saccharomyces cerevisiae* to select for gene deletions in actinomycetes. *Sci. Rep.* 4, 7100.
- (10) Urnov, F. D., Miller, J. C., Lee, Y. L., Beausejour, C. M., Rock, J. M., Augustus, S., Jamieson, A. C., Porteus, M. H., Gregory, P. D., and Holmes, M. C. (2005) Highly efficient endogenous human gene correction using designed zinc-finger nucleases. *Nature* 435, 646–651.
- (11) Boch, J., Scholze, H., Schornack, S., Landgraf, A., Hahn, S., Kay, S., Lahaye, T., Nickstadt, A., and Bonas, U. (2009) Breaking the code of DNA binding specificity of TAL-type III effectors. *Science* 326, 1509–1512.
- (12) Haft, D. H., Selengut, J., Mongodin, E. F., and Nelson, K. E. (2005) A guild of 45 CRISPR-associated (Cas) protein families and multiple CRISPR/Cas subtypes exist in prokaryotic genomes. *PLoS Comput. Biol.* 1, e60 DOI: 10.1371/journal.pcbi.0010060.
- (13) Barrangou, R., Fremaux, C., Deveau, H., Richards, M., Boyaval, P., Moineau, S., Romero, D. A., and Horvath, P. (2007) CRISPR provides acquired resistance against viruses in prokaryotes. *Science* 315, 1709–1712.
- (14) Bhaya, D., Davison, M., and Barrangou, R. (2011) CRISPR-Cas systems in bacteria and archaea: versatile small RNAs for adaptive defense and regulation. *Annu. Rev. Genet.* 45, 273–297.
- (15) Deveau, H., Garneau, J. E., and Moineau, S. (2010) CRISPR/Cas system and its role in phage-bacteria interactions. *Annu. Rev. Microbiol.* 64, 475–493.
- (16) Horvath, P., and Barrangou, R. (2010) CRISPR/Cas, the immune system of bacteria and archaea. *Science* 327, 167–170.
- (17) Jinek, M., Chylinski, K., Fonfara, I., Hauer, M., Doudna, J. A., and Charpentier, E. (2012) A programmable dual-RNA-guided DNA endonuclease in adaptive bacterial immunity. *Science* 337, 816–821.
- (18) Deltcheva, E., Chylinski, K., Sharma, C. M., Gonzales, K., Chao, Y. J., Pirzada, Z. A., Eckert, M. R., Vogel, J., and Charpentier, E. (2011) CRISPR RNA maturation by trans-encoded small RNA and host factor RNase III. *Nature* 471, 602–607.
- (19) Nishimasu, H., Ran, F. A., Hsu, P. D., Konermann, S., Shehata, S. I., Dohmae, N., Ishitani, R., Zhang, F., and Nureki, O. (2014) Crystal structure of Cas9 in complex with guide RNA and target DNA. *Cell* 156, 935–949.
- (20) Sternberg, S. H., Redding, S., Jinek, M., Greene, E. C., and Doudna, J. A. (2014) DNA interrogation by the CRISPR RNA-guided endonuclease Cas9. *Nature* 507, 62–67.
- (21) Hsu, P. D., Lander, E. S., and Zhang, F. (2014) Development and applications of CRISPR-Cas9 for genome engineering. *Cell* 157, 1262–1278.
- (22) DiCarlo, J. E., Norville, J. E., Mali, P., Rios, X., Aach, J., and Church, G. M. (2013) Genome engineering in *Saccharomyces cerevisiae* using CRISPR-Cas systems. *Nucleic Acids Res.* 41, 4336–4343.
- (23) Xie, K. B., and Yang, Y. N. (2013) RNA-guided genome editing in plants using a CRISPR/Cas System. *Mol. Plant* 6, 1975–1983.
- (24) Friedland, A. E., Tzur, Y. B., Esvelt, K. M., Colaiacovo, M. P., Church, G. M., and Calarco, J. A. (2013) Heritable genome editing in *C. elegans* via a CRISPR-Cas9 system. *Nat. Methods* 10, 741–743.
- (25) Bassett, A. R., Tibbit, C., Ponting, C. P., and Liu, J. L. (2013) Highly efficient targeted mutagenesis of *Drosophila* with the CRISPR/Cas9 system. *Cell Rep.* 4, 220–228.
- (26) Ronda, C., Pedersen, L. E., Hansen, H. G., Kallehauge, T. B., Betenbaugh, M. J., Nielsen, A. T., and Kildegaard, H. F. (2014) Accelerating genome editing in CHO cells using CRISPR Cas9 and CRISPy, a web-based target finding tool. *Biotechnol. Bioeng.* 111, 1604–1616.
- (27) Wang, H. Y., Yang, H., Shivalila, C. S., Dawlaty, M. M., Cheng, A. W., Zhang, F., and Jaenisch, R. (2013) One-step generation of mice carrying mutations in multiple genes by CRISPR/Cas-mediated genome engineering. *Cell* 153, 910–918.
- (28) Li, D. L., Qiu, Z. W., Shao, Y. J., Chen, Y. T., Guan, Y. T., Liu, M. Z., Li, Y. M., Gao, N., Wang, L. R., Lu, X. L., Zhao, Y. X., and Liu, M. Y. (2013) Heritable gene targeting in the mouse and rat using a CRISPR-Cas system. *Nat. Biotechnol.* 31, 681–683.
- (29) Yang, D. S., Xu, J., Zhu, T. Q., Fan, J. L., Lai, L. X., Zhang, J. F., and Chen, Y. E. (2014) Effective gene targeting in rabbits using RNA-guided Cas9 nucleases. *J. Mol. Cell Biol. (Oxford, U. K.)* 6, 97–99.
- (30) Mali, P., Yang, L., Esvelt, K. M., Aach, J., Guell, M., DiCarlo, J. E., Norville, J. E., and Church, G. M. (2013) RNA-guided human genome engineering via Cas9. *Science* 339, 823–826.
- (31) Cong, L., Ran, F. A., Cox, D., Lin, S., Barretto, R., Habib, N., Hsu, P. D., Wu, X., Jiang, W., Marraffini, L. A., and Zhang, F. (2013) Multiplex genome engineering using CRISPR/Cas systems. *Science* 339, 819–823.
- (32) Cobb, R. E., Wang, Y., and Zhao, H. (2014) High-efficiency multiplex genome editing of *Streptomyces* species using an engineered CRISPR/Cas system. *ACS Synth. Biol.*, DOI: 10.1021/sb500351f.
- (33) Qi, L. S., Larson, M. H., Gilbert, L. A., Doudna, J. A., Weissman, J. S., Arkin, A. P., and Lim, W. A. (2013) Repurposing CRISPR as an RNA-guided platform for sequence-specific control of gene expression. *Cell* 152, 1173–1183.
- (34) Wohlleben, W., Stegmann, E., and Süßmuth, R. D. (2009) Chapter 18. Molecular genetic approaches to analyze glycopeptide biosynthesis. *Methods Enzymol.* 458, 459–486.
- (35) Muth, G., Nussbaumer, B., Wohlleben, W., and Pühler, A. (1989) A vector system with temperature-sensitive replication for gene

disruption and mutational cloning in streptomycetes. *Mol. Gen. Genet.* 219, 341–348.

(36) Murakami, T., Holt, T. G., and Thompson, C. J. (1989) Thiostrepton-induced gene expression in *Streptomyces lividans*. *J. Bacteriol.* 171, 1459–1466.

(37) Yun, B. S., Hidaka, T., Kuzuyama, T., and Seto, H. (2001) Thiopeptide non-producing *Streptomyces* species carry the tipA gene: a clue to its function. *J. Antibiot.* 54, 375–378.

(38) Bowater, R., and Doherty, A. J. (2006) Making ends meet: repairing breaks in bacterial DNA by non-homologous end-joining. *PLoS Genet.* 2, e8 DOI: 10.1371/journal.pgen.0020008.

(39) Aravind, L., and Koonin, E. V. (2001) Prokaryotic homologs of the eukaryotic DNA-end-binding protein Ku, novel domains in the Ku protein and prediction of a prokaryotic double-strand break repair system. *Genome Res.* 11, 1365–1374.

(40) Smithies, O. (2001) Forty years with homologous recombination. *Nat. Med.* (N. Y., NY, U. S.) 7, 1083–1086.

(41) Xie, S. S., Shen, B., Zhang, C. B., Huang, X. X., and Zhang, Y. L. (2014) sgRNAs9: A software package for designing CRISPR sgRNA and evaluating potential off-target cleavage sites. *PLoS One* 9, e100448 DOI: 10.1371/journal.pone.0100448.

(42) Iliakis, G., Wang, H., Perrault, A. R., Boecker, W., Rosidi, B., Windhofer, F., Wu, W., Guan, J., Terzoudi, G., and Pantelias, G. (2004) Mechanisms of DNA double strand break repair and chromosome aberration formation. *Cytogenet. Genome Res.* 104, 14–20.

(43) Kanaar, R., Hoeijmakers, J. H., and van Gent, D. C. (1998) Molecular mechanisms of DNA double strand break repair. *Trends Cell Biol.* 8, 483–489.

(44) Citorik, R. J., Mimee, M., and Lu, T. K. (2014) Sequence-specific antimicrobials using efficiently delivered RNA-guided nucleases. *Nat. Biotechnol.* 32, 1141–1145.

(45) Jiang, W. Y., Bikard, D., Cox, D., Zhang, F., and Marraffini, L. A. (2013) RNA-guided editing of bacterial genomes using CRISPR-Cas systems. *Nat. Biotechnol.* 31, 233–239.

(46) Gomaa, A. A., Klumpe, H. E., Luo, M. L., Selle, K., Barrangou, R., and Beisel, C. L. (2014) Programmable removal of bacterial strains by use of genome-targeting CRISPR-Cas systems. *mBio* 5, e00928-13 DOI: 10.1128/mBio.00928-13.

(47) Bikard, D., Euler, C. W., Jiang, W. Y., Nussenzweig, P. M., Goldberg, G. W., Duportet, X., Fischetti, V. A., and Marraffini, L. A. (2014) Exploiting CRISPR-Cas nucleases to produce sequence-specific antimicrobials. *Nat. Biotechnol.* 32, 1146–1150.

(48) Rudolph, M. M., Vockenhuber, M. P., and Suess, B. (2013) Synthetic riboswitches for the conditional control of gene expression in *Streptomyces coelicolor*. *Microbiology (Reading, U. K.)* 159, 1416–1422.

(49) Uguru, G. C., Mondhe, M., Goh, S., Hesketh, A., Bibb, M. J., Good, L., and Stach, J. E. M. (2013) Synthetic RNA silencing of actinorhodin biosynthesis in *Streptomyces coelicolor* A3(2). *PLoS One* 8, e67509 DOI: 10.1371/journal.pone.0067509.

(50) Wu, H., Wang, Y., Wang, Y., Cao, X., Wu, Y., Meng, Z., Su, Q., Wang, Z., Yang, S., Xu, W., Liu, S., Cheng, P., Wu, J., Khan, M. R., He, L., and Ma, G. (2014) Quantitatively relating gene expression to light intensity via the serial connection of blue light sensor and CRISPRi. *ACS Synth. Biol.* 3, 979–982.

(51) Gilbert, L. A., Horlbeck, M. A., Adamson, B., Villalta, J. E., Chen, Y., Whitehead, E. H., Guimaraes, C., Panning, B., Ploegh, H. L., Bassik, M. C., Qi, L. S., Kampmann, M., and Weissman, J. S. (2014) Genome-scale CRISPR-mediated control of gene repression and activation. *Cell* 159, 647–661.

(52) Takano, E., White, J., Thompson, C. J., and Bibb, M. J. (1995) Construction of thiostrepton-inducible, high-copy-number expression vectors for use in *Streptomyces* spp. *Gene* 166, 133–137.

(53) Bentley, S. D., Chater, K. F., Cerdeno-Tarraga, A. M., Challis, G. L., Thomson, N. R., James, K. D., Harris, D. E., Quail, M. A., Kieser, H., Harper, D., Bateman, A., Brown, S., Chandra, G., Chen, C. W., Collins, M., Cronin, A., Fraser, A., Goble, A., Hidalgo, J., Hornsby, T., Howarth, S., Huang, C. H., Kieser, T., Larke, L., Murphy, L., Oliver, K.,

O'Neil, S., Rabinowitz, E., Rajandream, M. A., Rutherford, K., Rutter, S., Seeger, K., Saunders, D., Sharp, S., Squares, R., Squares, S., Taylor, K., Warren, T., Wietzorrek, A., Woodward, J., Barrrell, B. G., Parkhill, J., and Hopwood, D. A. (2002) Complete genome sequence of the model actinomycete *Streptomyces coelicolor* A3(2). *Nature* 417, 141–147.

(54) Li, H., and Durbin, R. (2009) Fast and accurate short read alignment with Burrows–Wheeler transform. *Bioinformatics* 25, 1754–1760.

(55) Hilker, R., Stadermann, K. B., Doppmeier, D., Kalinowski, J., Stoye, J., Straube, J., Winnebal, J., and Goesmann, A. (2014) ReadXplorer—visualization and analysis of mapped sequences. *Bioinformatics* 30, 2247–2254.

(56) Rutherford, K., Parkhill, J., Crook, J., Horsnell, T., Rice, P., Rajandream, M. A., and Barrrell, B. (2000) Artemis: sequence visualization and annotation. *Bioinformatics* 16, 944–945.

(57) Bystrykh, L. V., Fernandez-Moreno, M. A., Herrema, J. K., Malpartida, F., Hopwood, D. A., and Dijkhuizen, L. (1996) Production of actinorhodin-related “blue pigments” by *Streptomyces coelicolor* A3(2). *J. Bacteriol.* 178, 2238–2244.

(58) Craney, A., Ahmed, S., and Nodwell, J. (2013) Towards a new science of secondary metabolism. *J. Antibiot.* 66, 387–400.

■ NOTE ADDED AFTER ASAP PUBLICATION

This paper was published ASAP on April 7, 2015, with incorrect data in the Supporting Information Tables S2, S3, and S5. The corrected version was reposted on August 21, 2015.